The Development of Advanced Materials - High Performance Properties of Composite for Automotive and Aerospace Applications

Jamaliah Idris[1], J.C.Tan[2] & C.W.Chang

Faculty of Mechanical Engineering, Universiti Teknologi Malaysia,
81310 Skudai, Johor, Malaysia

ABSTRACT

Magnesium metal matrix composite (MMC) is an excellent candidate for moving engine components and airframes due to its low density. Magnesium's lightweight and natural affinity for wetting to ceramic particle reinforcements such as silicon carbide (SiC) make it one of the best choices as a matrix metal. However, magnesium alone without reinforcement is not suitable for mechanical applications due to its low wear resistance performance. The magnesium matrix composites used in this study were produced by powder metallurgy technique. The wear resistance of SiC_p/AZ91 composite reinforced with 0, 5, 10, 15 and 20 wt.% SiC were studied. Pin-on-disk dry sliding wear tests were carried out to study the volumetric wear, wear rate and wear mechanisms. The magnesium matrix composites were used as pins while the counterface consisted of mild steel disks. Worn surfaces of pins and the wear debris were investigated by using Scanning Electron Microscopy (SEM) and Energy Dispersive X-Ray Analysis (EDX). The wear resistance performance of magnesium matrix composites was found to improve with increasing volume fraction of SiC. Volumetric wear was found to increase with sliding distance and the wear rate was greatly reduced after the wear-in phenomenon. For AZ91 Mg-SiCp/ steel dry sliding wear system, 20-wt.% SiC_p/AZ91 magnesium composite was found to have the best wear resistant performance. During the wear-in period, abrasion was predominant during the wear-in stage. In the corrosion study, corrosion behavior of Mg-based metal matrix composites SiC particulate reinforced AZ91 (SiC/AZ91) with reinforcement weight fraction of 5, 10, 15 and 20 wt.% as well as the monolithic AZ91 alloy was studied. The galvanic effect of SiC reinforcement on the matrix alloy was also investigated. The studies were carried out under temperature of $30° ± 1°C$ and pH 7 in aerated 0.1 M NaCl solution. The materials were studied by using electrochemical corrosion test, weight-loss measurement of corrosion rate, elemental analysis, X-ray diffraction and microscopic examination. The corrosion rates of the composites increased with the increase of SiC weight fraction. The significance of galvanic effect of SiC on the matrix alloy was proven where intersection of superimposed Tafel curves between sintered SiC and monolithic AZ91 occurred at higher corrosion current density (i_{corr}) and lower corrosion potential (E_{corr}). The corrosion was found localized at low SiC weight fraction, and gradually change to general corrosion. The corrosion rates of the composites were at least three times higher than the monolithic AZ91, due to galvanic effect of SiC on the matrix alloy and detachment of SiC particles from the materials.

Keywords: Advanced materials, high performance properties, automotive

INTRODUCTION

The development of enhanced strength magnesium alloys and the concurrent interest in research into this field, suggesting magnesium metal matrix composites (MMCs) use for a variety of aeronautical, automotive and other advanced engineering applications (Baker 1989). Magnesium has been used for automotive components such as clutch housing, wheels and cylinder heads. However, magnesium's usage is still limited to applications that do not involve sliding surfaces because of its poor wear resistance. Although wear resistance of magnesium can be improved by using conventional methods

like chrome or nickel plating, carburising and nitriding, these methods will lead to a higher finishing cost (Mikucki *et al.* 1986).

Previous experimental studies have shown that the abrasive wear resistance performance of metal matrix composites increased with increasing volume fraction of the particle reinforcement content. It is also found that various factors such as particles size, shape, volume fraction can affect the wear resistance performance of MMCs (Wang *et. al.* 1991). However, when a metallic material is chosen as the wear counterface, some researchers have found that the sliding wear resistance of metal matrix composites will decrease with increasing particle volume fraction (Alpas 1991). Hence, different wear counterfaces can result in different wear mechanisms and wear behaviour. The study of MMCs/steel wear systems is essential due to the increase in the number of steel or steel alloy components used as wear counterfaces in tribosystems (Zhang 1995).

Research conducted on the wear resistance performance of magnesium metal matrix composites against a metallic counterface is sparse. Therefore, in this paper, the sliding wear resistance of AZ91 Mg-SiCp/ steel dry sliding wear system has been studied. The various wear mechanisms is also investigated.

The corrosion rate of magnesium is highly dependent on its purity. In seawater, ultrapure magnesium corrodes at a rate of 0.25mm/year. However, commercial magnesium corrodes about 100-500 time faster (Uhlig 1985). The higher corrosion rate of commercial magnesium is primarily caused by noble impurity elements which have low hydrogen overvoltages, such as iron, nickel, cobalt and copper (Allan 1987). Besides, corrosion rate can be high in acidic or neutral solutions where magnesium does not passivate (Hihara 1994). At pH level greater than about 8.5, magnesium passivates by the formation of a $Mg(OH)_2$-film (Muylder 1974), and is, therefore, resistant to alkalies. Magnesium is resistant to dilute alkalies and 50% caustic liquors below 60°C, but the corrosion rate increases rapidly with temperatures above 60°C. Corrosion and pitting increase as temperature increases when cathodic impurities are present in amounts greater than their tolerance value.

EXPERIMENTAL PROCEDURE

The magnesium matrix composites being investigated consist of magnesium AZ91 reinforced with 0 wt.% (monolithic AZ91), 5, 10, 15 and 20 wt.% of SiC particles. These SiC_p/AZ91 composites were produced by Japan Mechanical Laboratory (MEL), through powder metallurgy technique. The average size of the atomised AZ91 magnesium powder used was 14μm while average size for SiC particle was 0.5μm. Tables 1 and 2 show the chemical composition of AZ91 powder and SiC particles respectively.

TABLE 1				
Chemical composition of AZ91 powder				
Al	Zn	Si	Cu	Mg
9.0	0.8	0.1	0.05	Bal.

TABLE 2				
Chemical composition of SiC particles				
Al	Fe	Free C	Free SiO_2	SiC
0.01	0.03	0.78	0.28	Bal.

The hot extruded SiCp/AZ91 composite blanks 9mm were machined into cylindrical pin samples with a diameter of 6mm and length of 10mm. The Vickers microhardness of the matrix was measured under a load of 500g with a loading time of 15s. Five readings were taken and their respective average hardness is calculated, given in Table 3.

TABLE 3
Vickers hardness of magnesium matrix composites.

Wt.% SiC	0%	5%	10%	15%	20%
Hv	82	111	127	148	170

The counterface material used was mild steel with an average hardness of 135 Hv. The surfaces of the pins and disks were polished to 1μm. Before the wear tests, the surface morphology of the mating surfaces was studied with optical microscope.

Dry sliding wear tests were conducted on a *Cygnus* pin-on-disk wear-testing machine based on ASTM-G99 standard. Three composite pins were mounted in the pin holder and were held against a rotating mild steel disk. Prior to the test, surfaces of the pin and disk were cleaned with acetone. All tests were carried out at a fixed track diameter of 70mm and at a constant sliding speed of $0.37ms^{-1}$ (100RPM). The weight on the load arm extension rod was adjusted to give the required test load of 90N. This load gave a normal stress of 1.06MPa on each pin. The sliding distance was set at 1000m. Each test was done using a new steel disk.

During the tests, an inductive probe that was in contact with the face of a micrometer was utilised to measure the cumulative linear pin wear (mm). Samples were tested twice at each condition and the average values of cumulative pin wear was calculated from six specimens. The volumetric wear and wear rates were given by the following equations:

$$\text{Wear volume} = \text{Linear wear (mm)} \times \text{Cross section of pin (mm}^2)$$

$$\text{Wear rate} = \frac{\text{Wear volume (mm}^3)}{\text{Sliding Distance (m)}}$$

After the wear tests, the worn surfaces of the composite pins and wear debris were investigated by using scanning electron microscopy (SEM) and energy dispersive X-ray analysis (EDX).

Tafel Extrapolation Test and Immersion Corrosion Test are the testing methods that have been used to study the corrosion behaviour of Mg MMC. The Tafel Test is conducted by using the GAMRY CMS105 corrosion cell. The experimental procedure follows the standard recommended practice in ASTM G5-78 with air-exposed 0.1 M NaCl as electrolyte at room temperature (30°C ± 1°C) and at pH 7. A saturated calomel electrode is used as the standard electrode and graphite as the auxiliary electrode. Cell current is measured during a slow sweep of the potential. The immersion corrosion test was conducted by weight-loss method, following the standard practice of ASTM G31-72 in air-exposed 0.1 M NaCl at room temperature (30°C ± 1°C) and at pH 7. Changes in the solution corrosivity and composites corrodibility (corrosion rate) with time are determined with a *planned interval* testing program (Jones 1992). A simplified immersion test is used by suspending the specimens in a beaker filled with solution in ambient atmosphere. Circular specimens of about 8.7mm diameter were prepared, with thickness of 4 mm, 3 mm drilled hole for mounting purpose and final surface finish with 150-grit SiC paper. Cleaning procedure for the corroded specimens follows the standard practice of ASTM G1-81 using chromic acid solution.

Jamaliah Idris, J.C. Tan & C.W. Chang

RESULTS AND DISCUSSION

Wear Tests Results

Figure 1 shows the volumetric wear of magnesium composites while Figure 2 depicts their wear rates throughout the 1000m sliding distance.

Magnesium metal matrix composites exhibited lower volumetric wear as well as lower wear rate compared to unreinforced magnesium alloy throughout the 1000m sliding distance. When the SiC content was increased from 0 wt.% to 5, 10, 15 and 20 wt.%, the wear resistance performance of the composite was gradually improved. Hence, when SiC content is increased the wear resistance performance of magnesium composite becomes more significant and superior. One explanation for this is that the hardness of magnesium composite increases when the amount of SiC reinforcement is increased, as shown in Table 3. Magnesium matrix composite with a higher hardness number has greater resistance against wear.
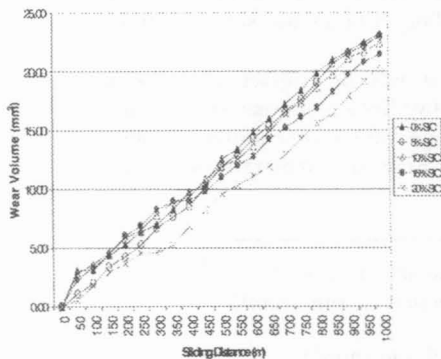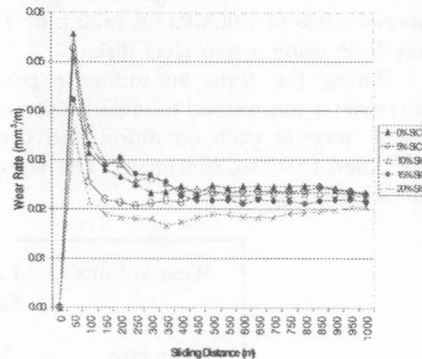

Fig. 1. Volumetric wear (mm3) vs.
sliding distance (m)

Fig. 2. Wear rate (mm3/m) vs.
sliding distance (m)

From Figure 1, it can be observed that the improvement in wear resistance of the 5 wt.% SiC_p/AZ91 composite over the unreinforced AZ91 magnesium alloy is not very significant. It can be assumed that the 5 wt.% of SiC reinforcement is still insufficient to effectively protect the soft magnesium matrix against wear on a steel counterface. It is also found that 20 wt.% SiC/AZ91 composite offers the best wear resistance performance throughout the 1000m sliding distance.

The hard SiC particles protect the softer AZ91 alloy from sliding wear. They act as the major load- bearing element for the composite. At low loads, the composites achieve their wear resistance properties from SiC reinforcing particles. Under higher loads, the reinforcement particles will fracture, as shown in Figure 3. The fractured particles will lose their ability to carry load exerted upon them. However, the fractured particles might also form a layer of comminuted phase, which provide protection against seizure (ZumGahr 1987). Formation of this layer can reduce friction and hence increase wear resistance.

The shape and size of SiC particles have a major influence on wear resistance of magnesium matrix composites. Improvement in wear resistance may be due to the fine size of the SiC particles used i.e. about 0.5 mm. Fine particles contribute more towards the improvement of the wear resistance of magnesium matrix composites compared to larger reinforcement particles (Hutchings 1994). This is because finer particles are
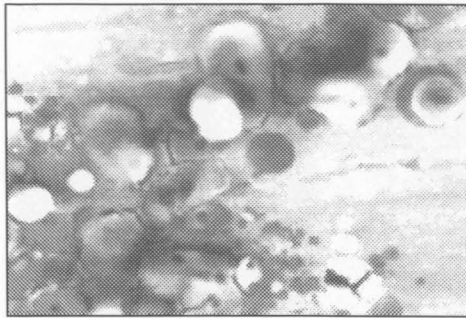
Fig. 3. Fractured SiC particles – 15% SiCp/AZ91

distributed more uniformly throughout the matrix and hence the composite will have more uniform deformation when loaded.

The graph of wear rate vs. sliding distance (Figure 2) shows very high wear rates for all the composites at the initial stage of the test. There was a sudden increase of wear rates during the initial 50m of sliding distance. The slope of the graph within this 50m of sliding is very much steeper than the later stage of sliding. Within this initial 50m, the contacting surfaces of the specimens were 'worn-in'. Since this was a dry sliding wear test, the high frictional force that acted between the composite pin surface and the steel counterface had accelerated this 'wear-in' phenomenon.

After the 'wear-in', wear rates decreased gradually and remained at a rather constant value until the end of the 1000m sliding distance. This indicates steady state wear was achieved when the sliding distance exceeded 250m. The slope of the volumetric wear vs. sliding distance graph (Figure 1) slightly decreases during steady state wear, which means that volumetric wear was reduced. This phenomenon is true for all the specimens tested under the AZ91 Mg-SiC$_p$/steel dry sliding wear system.

Abrasive wear takes place during the wear-in stage. During the initial 50m of sliding distance, a high volumetric wear and wear rate was observed, as shown in Figures 1 and 2. During the wear-in, a high volume of material is quickly abraded by the hard asperities on the hard surfaces (Zhang 1995). Within this sliding distance, abrasion is the predominant wear mechanism. The volumetric wear of the magnesium composite pin increased steeply and then reduced to a lower value. Wear-in took place until a steady state was reached, which was found to be after 250m of sliding distance.

Abrasive wear is indicated by the parallel and continuous scratches that exist on the worn surfaces as shown in Figure 4. Deep parallel grooves and cavities can be seen on the abraded surface. Cavities were produced by the fracture of ceramic particles or by the ploughing of hard particles. An example of surface ploughing is shown in Figure 5. The high volumetric wear during the wear-in was due to the protruding SiC particles (Figure 6) which acted as cutting tools to scratch the steel surface and form rough grooves. At the same time, the steel asperities abraded the matrix alloy to form grooves on the composite surface. There were also ceramic particles that were fractured and embedded on the steel surface resulting in extra scratching on the composite.

EDX analysis had indicated that the wear debris both came from the composite and the steel disk. Particle fracture and inter-particle fracture can be observed from SEM photomicrographs, as shown in Figure 3. Fractured ceramic particles will form loose particles that lead to three-body abrasion mechanism that can reduce the wear rate. This is because the presence of loose particles can reduce metal to metal contact.
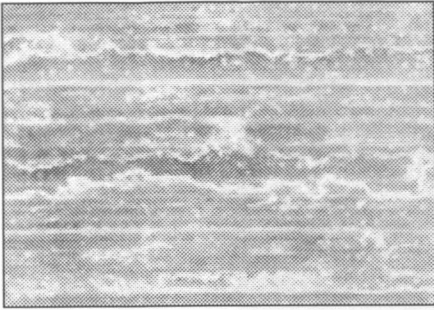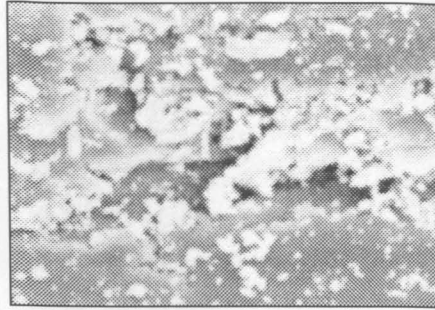
Fig. 4. Abrasion grooves – 10% SiCp/AZ91

Fig. 5. Surface ploughing – 10% SiCP/AZ91

Fig. 6. Protruding SiC particles – 15%
SiC_p/AZ91

The strength of bonding and particle-matrix interface plays a vital role in determining whether the fractured particles will remain attach to the matrix. Good interface and strong bonding will not produce voids since SiC particles although fractured still attach to the matrix. This can be observed in Figure 3.

Corrosion Behaviour:
Tafel Extrapolation Test

The data being logged during the experiment was E_{corr} and i_{corr}, whereas the analyzed result was corrosion penetration rate (CPR) in term of mils per year (mpy). Figure 7 shows the result for 5 wt.% SiC/AZ91. Figure 7: Tafel curve for 5 wt.% SiC/AZ91

The Tafel extrapolation results show the corrosion current density of the materials (in A/cm²) increases with the increase of the reinforcement weight percentage. From Figure 8, it is expected that the corrosion rate will continue to increase for higher weight percent of reinforcement.

The superimposed Tafel curve for monolithic AZ91 and 5 wt.% SiC/AZ91 shows that composite has lower corrosion potential and higher corrosion current density or corrosion rate compared to alloy. The monolithic AZ91 alloy has slightly higher corrosion potential compared to the SiC/AZ91 composites. This is because the composites content AZ91 alloy as matrix and SiC as reinforcement. SiC is a stable material that has low corrosion potential and low corrosion rate. When SiC is galvanically coupled with AZ91 alloy, lower corrosion potential is expected according to *Mixed Potential Theory*. It is obvious from the results that the current density and the corrosion rate increase with
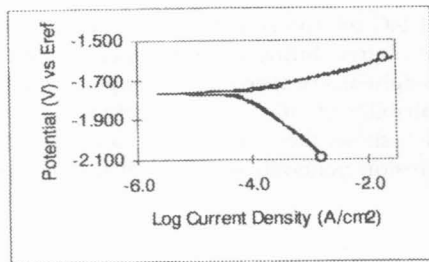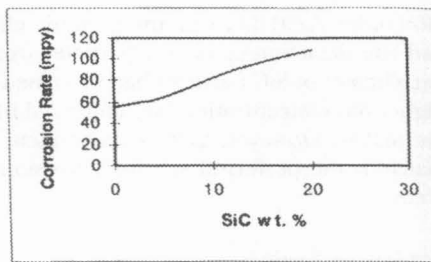
Fig. 7. Tafel curve for 5 wt. % SiC/AZ91

Fig. 8. Corrosion rate vs. SiC wt.%

the increase of reinforcement weight percent. The existence of SiC particulates at the exposing surface of SiC/AZ91 during the Tafel test has reduced the effective area for equivalent exchange compared to monolithic AZ91. Meanwhile, the presence of SiC in the composite as cathodic material will shift the corrosion nature of AZ91 to more anodic region compared to monolithic AZ91 alloy. This causes the matrix to dilute faster in the solution with higher corrosion current density. By applying the *Mixed Potential Theory*, at higher SiC to AZ91 ratio, lower corrosion potential and higher current density can be obtained. It explains the results of Tafel extrapolation tests where the corrosion rate of SiC/AZ91 increases with the increase of reinforcement weight percent.
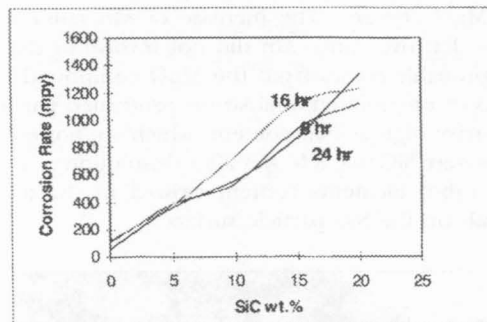

Fig. 9. Corrosion rate vs. immersion period.

Immersion Corrosion Test

During the immersion process, odourless gas evolution was observed for all specimens. Gray coloured corrosion products were observed at the bottom of containers for the composite specimens. The relationship between the corrosion rate and reinforcement weight fraction of the materials is shown in Figure 9. The corrosion rates of all the specimens increase with the increase of SiC weight percent and have maximum corrosion rate at 16th hours of immersion, except for 20 wt.% SiC/AZ91 which occurred at 24th hour of immersion. The 20 wt.% SiC/AZ91 had its corrosion rate increased continuously over the immersion period. It is suspected that pitting dominates the corrosion behavior of monolithic AZ91 and composites with reinforcement lower than 20 wt.%, but for 20 wt.% SiC/AZ91 corrosion occurred by general corrosion. Since the comparison with the control specimen shows that corrodibility for specimen and solution corrosiveness decreased, it is expected that further immersion may decrease the corrosion rate. The corrosion rates of the composites were found higher than the

monolithic AZ91 because the galvanic effect of SiC reinforcement on the matrix alloy and the detachment of SiC particles from the matrix during corrosion process. The detachment of SiC particles had increased the weight-loss of specimens. Composites with higher SiC concentration had increased the probability of SiC particle detachment from the matrix. However, there is no evidence which shows that the interface area of SiC-matrix is the preferred site for corrosion. Corrosion generally occurred at the matrix areas.

Composition Analysis

The composition analysis of corroded specimens was done by using EDX analyzer and X-ray Diffractometer (XRD). The EDX analyses focus on the corroded specimens for elemental analysis of corrosion products and to investigate the changes of composition of the residue material after 8 hours of immersion. Whereas the XRD is used to check the composition of the insoluble corrosion products collected by filtration of solution after immersion corrosion test. Figure 10 shows the SEM micrograph for 20 wt.% SiC/ AZ91 corroded specimen after 8 hours of immersion. EDX analysis was carried out at protruded particle. The composition of the specimens does not change with corrosion. The Mg content drops and Si content increases over a wide range when the overall analysis results are compared to the pin-pointed results. From the qualitative analysis by using X-ray Diffractometer (XRD), the main compound found in the corrosion products was SiC. From the average EDX analysis, the only difference that can be observed is the increase of Mn and MgO content. The increase of Mn content is probably due to material that had been left over since Mn did not involve in the corrosion reactions. Whereas the oxygen probably comes from the MgO compound that attached on the specimens. The results of pin-pointed analysis on protruded particles attached on the matrix show extraordinary high silicon content, which supported the assumption that the protruded particles were SiC that left over after dissolution of surrounding interfacial matrix. The Mg and other elements content existed in the analysis were probably residue matrix materials on the SiC particle surface.
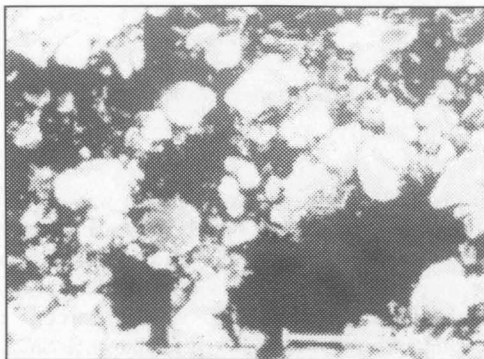
Fig. 10. SEM micrograph of 20 wt% SiC/AZ91 after
8 hours of corosion (5000X)

CONCLUSIONS

The following conclusions are drawn from the sliding and corrosion test for AZSI Mg - SiC$_p$ composite matrix:

1. Volumetric wear increases with sliding distance and the wear rate is greatly reduced after the wear-in phenomenon.
2. Wear resistance performance of magnesium matrix composites increases with increasing volume fraction of SiC reinforcement. Higher SiC volume fraction will produce harder composites which are more wear resistant.
3. During the wear-in period, abrasion is predominant.
4. The weight fraction of SiC reinforcement is proportional to the corrosion rate of the composite. The presence of SiC reinforcement shifts the matrix to more anodic region and causes it to dilute faster.
5. The SiC reinforcement reduces the effective area for equivalent exchange and caused higher corrosion rate of the composite.
6. Higher reinforcement to matrix alloy ratio enhances galvanic effect of SiC on the matrix alloy and causes the composite to have higher corrosion current density according to *Mixed Potential Theory*.
7. As the reinforcement weight fraction increases (ie., up to 20 wt.%) corrosion mechanism changes from pitting to general corrosion.

ACKNOWLEDGEMENT

REFERENCES

ALLAN, F. *et al.* 1987. Corrosion Of Magnesium And Magnesium Alloys. In *Metal Handbook*, Vol. 3 : Corrosion. Ohio : ASM International Handbook Committee.

ALPAS A.T. and J.D. EMBURY. 1985. *Wear of Materials*, p.784-93. ASME, New York.

BAKER, H. 1989. Adv. Materials and Processes. Pg.35. Sept.

BALASUBRAMANIAN, P.K. et al. 1990. Solidification of Metal Matrix Composites. Indianapolis : Metals and Materials Society.

BRIAN, T. and J. GLYN. 1990. *Metal Matrix Composites : Current Developments and Future Trends in Industrial Research and Application*. England : Elsevier Science Publishers Ltd.

FONTANA M.G. 1986. Corrosion Engineering. Pg. 462-463, 482- 504. Singapore: McGraw-Hill Book Company, Inc.

HIHARA L.H. and P.K. KONDEPUDI. 1993. Galvanic corrosion between SiC Monofilament and Magnesium in $NaCl$, Na_2SO_4 and $NaNO_3$ solutions for application to metal matrix Composites. *Corrosion Science*, **36**: 1585-1595. 1994.

HIHARA L.H. and R.M. LATANISION. 1994. Corrosion of metal matrix composite. *International Materials Reviews* **39**: 245-262.

HUTCHINGS, I.M. 1994. Tribological properties of metal matrix composites. *Materials Science and Technology* **10**: 513-517

JONES D.A. 1992. *Principles and Prevention of Corrosion*. Pg: 75-76. New York: McMillan Publishing Company.

LUO A. 1994. Processing, microstructure and mechanical behavior of magnesium metal matrix composites. *Metallurgical and Materials Transactions* A, **26A**: 2445-2454. 1995.

Mickucki, B.A. et al. 1986. Ceramic strengthen magnesium. *Materials Engineering* **103**: 60.

Muylder, J.V. and M. Pourbaix. 1974. Atlas of Electrochemical Equilibria. In *Aqueous Solution*. Houston : National Association of Corrosion Engineers.

Pourbaix M. 1973. *Lectures on Electrochemical Corrosion*. Pg: 67-83. New York: Plenum Press.

Purazrang, K., P. Abachi and K.U. Kainer. 1994. Investigation of the mechanical behaviour of magnesium composites. *Composites* **25**(4): 296- 302.

Schwartz, M.M. 1997. *Composites Materials : Processing, Fabrication And Applications*. Vol. 2. New Jersey : Prentice Hall.

Uhlig, H.H. and R.W. Revie. 1985. *Corrosion and Corrosion Control*. New York : John Wiley.

Wachter, A. and R.S. Treseder. 1947. Corrosion testing evaluation of metals for process equipment. *Chemical Engineering Progress* **43**: 315-326.

Wang, Aiguo and H. J. Rack. 1991. Dry sliding wear in 2124 Al-SiCw/17-4 PH stainless steel systems. Wear. Pg.354

Zhang Z. F., L. C. Zhang and Y. W. Mai. 1995. Wear of ceramic particle-reinforced metal-matrix composites, Part I: Wear mechanisms. *Journal of Materials Science* **30**: 1961-1966.

ZumGahr K. H. 1987. *Microstructure and Wear of Materials*. Elsevier, Amsterdam.